Journal of Molecular Catalysis A: Chemical 304 (2009) 107–116

Contents lists available at ScienceDirect

Journal of Molecular Catalysis A: Chemical

journal homepage: www.elsevier.com/locate/molcata

MCM-41/*ansa*-zirconocene supported catalysts: Preparation, characterization and catalytic behaviour in ethylene polymerization

Carlos Alonso-Moreno, Damián Pérez-Quintanilla, Dorian Polo-Cerón, Sanjiv Prashar*, Isabel Sierra*, Isabel del Hierro, Mariano Fajardo

Departamento de Química Inorgánica y Analítica, E.S.C.E.T., Universidad Rey Juan Carlos, 28933 Móstoles (Madrid), Spain

ARTICLE INFO

Article history:
Received 6 May 2008
Received in revised form 25 January 2009
Accepted 29 January 2009
Available online 7 February 2009

Keywords:
Mesoporous silica
Metallocene complexes
Supported catalysts
Polymerization

ABSTRACT

An MCM-41 has been modified by grafting several zirconocene complexes to give new materials potentially active in the polymerization of α-olefins. These materials have been activated by the cocatalyst MAO, to generate the catalysts MCM-41/metallocene/MAO (metallocene = [Zr(η^5-C_5H_5)$_2$Cl$_2$] (**1**), [Zr{Me$_2$Si(η^5-C_5Me_4)(η^5-C_5H_4)}Cl$_2$] (**2**) and [Zr{Me$_2$Si(η^5-C_5Me_4)(η^5-$C_5H_3Bu^t$)}Cl$_2$] (**3**)). The resulting functionalized ordered mesoporous silica samples (**1**–**3**) were tested as catalysts in the polymerization of ethylene and compared with both the homogeneous system analogues and the functionalized silica derivatives SG/metallocene/MAO (SG = silica gel; metallocene = [Zr(η^5-C_5H_5)$_2$Cl$_2$] (**4**), [Zr{Me$_2$Si(η^5-C_5Me_4)(η^5-C_5H_4)}Cl$_2$] (**5**) and [Zr{Me$_2$Si(η^5-C_5Me_4)(η^5-$C_5H_3Bu^t$)}Cl$_2$] (**6**)). The metallocenes **2** and **3** have been characterized by ^{13}C-CP MAS NMR and ^{29}Si MAS NMR spectroscopy. The structure and surface properties of MCM-41/[Zr{Me$_2$Si(η^5-C_5Me_4)(η^5-C_5H_4)}Cl$_2$] and MCM-41/[Zr{Me$_2$Si(η^5-C_5Me_4)(η^5-C_5H_4)}Cl$_2$]/MAO systems have been studied by X-ray diffractometry, nitrogen adsorption–desorption isotherms measurement and thermogravimetry. The grafting of the metallocene complexes, activation with MAO and subsequent polymerization reaction have been followed by an FT-IR "in situ" study. Scanning electron microscopy and transmission electron microscopy have been used to show the morphology of the heterogeneous catalysts as well as the resulting polyethylene obtained.

1. Introduction

New mesoporous materials with a large BET surface area, high porosity, controllable and narrowly distributed pore sizes and ordered pore arrangements are known to be promising candidates for use in catalysis [1]. These properties are already of great utility for producing carriers on which catalytically active species such as transition metal complexes can be supported [2].

Since the initial reports in 1957 of homogeneous catalysts for alkene polymerization [3], there has been an expanding interest in the application and evolution of new catalytic systems [4]. Amongst these, metallocene/MAO catalytic systems are highly efficient in producing polyolefins with defined microstructures and narrow molecular weight distributions [5], although to date, these systems have generally been applied in solution. However, for most industrial applications, it is desirable to employ these catalysts in gas phase reactions in order to take advantage of existing heterogeneous polymerization plant infrastructure and thus avoiding costly modifications needed in incorporating homogeneous systems. The single-site catalysts therefore need to be immobilized on a solid support in order to be active in gas phase processes.

The most common method of employing metallocene compounds in heterogeneous polymerization is to support the complexes on inorganic solids (in most cases silica gel) [6]. There are four different routes to supported catalysts: (i) direct adsorption of the metallocene on the carrier surface leading to physisorption or chemisorption of the metallocene complex (direct heterogenization); (ii) direct adsorption of the metallocene/MAO adduct on the support; (iii) initial adsorption of MAO to the support followed by adsorption of the metallocene complex (indirect heterogenization); (iv) covalent bonding between the ligands of the metallocene complex and the carrier surface followed by activation with external MAO.

Lower yields and catalytic activity compared with homogenous systems are still the most important problems that need to be overcome when using heterogeneous catalysts [7] and are attributed to the steric hindrance around the active site on the silica surface [8].

Mesoporous silicas, such as MCM-41, belong to the family of mesoporous molecular sieves with hexagonal ordered pores. MCM-41 silica is well-known for their crystalline structures with narrow pore size distribution and large surface area [9]. MCM-41 has been observed suppressing the formation of inactive binuclear complexes between two metallocene units or between metallocene and

* Corresponding authors. Tel.: +34 914887186; fax: +34 914888143.
E-mail addresses: sanjiv.prashar@urjc.es (S. Prashar), isabel.sierra@urjc.es (I. Sierra).

1381-1169/$ – see front matter © 2009 Elsevier B.V. All rights reserved.
doi:10.1016/j.molcata.2009.01.034

methylaluminoxane fragments, thus giving stable active sites for olefin polymerization [10].

Here, as a part of our ongoing studies in the design of olefin polymerization catalysts in both homogeneous [11] and heterogeneous [12] systems and the preparation of new mesoporous materials with important applications [13], we have prepared and characterized MCM-41 with supported *ansa*-zirconocene complexes and studied their catalytic behaviour in ethylene polymerization. The reasoning behind using *ansa*-metallocene systems in this study is that under homogeneous conditions, these catalysts are known to offer a much higher degree of selectivity in α-olefin polymerization with respect to their unbridged counterparts [11].

2. Experimental

2.1. Materials

All manipulations were performed under dry nitrogen gas using standard Schlenk techniques. Toluene was purified by distillation under nitrogen from sodium (low-sulphur toluene). Silica gel (SG) with a specific area (S_{BET}) of 500 m^2/g and an average pore diameter of 60 Å (Sigma–Aldrich, Germany) was dried under vacuum (10^{-2} mmHg) for 16 h at 500 °C, cooled and stored under dry nitrogen. MCM-41 was prepared according to the method of Landau et al. using a hydrothermal crystallization, and dried under vacuum (10^{-2} mmHg) for 16 h at 500 °C, cooled and stored under dry nitrogen [14]. [Zr(η^5-C_5H_5)$_2$$Cl_2$] (Strem), ethylene (Air Liquide), $AlBu^i_3$ (TIBA, Aldrich) and MAO (Aldrich) were used without further purification. [Zr{Me_2Si(η^5-C_5Me_4)(η^5-C_5H_4)}Cl_2] and [Zr{Me_2Si(η^5-C_5Me_4)(η^5-$C_5H_3Bu^t$)}Cl_2] were prepared according to the literature procedures [15].

2.2. Preparation of the modified surfaces

2.2.1. MCM-41/[Zr(η^5-C_5H_5)$_2$$Cl_2$]/MAO (**1**)

The modified mesoporous surface **1** was prepared under an inert atmosphere using Schlenk techniques and a glove-box. A solution of [Zr(η^5-C_5H_5)$_2$$Cl_2$] (32 mg, 0.11 mmol) (to obtain a theoretical level of 1% Zr/SiO_2) in toluene (30 ml) was added to MCM-41 (1.00 g) and the mixture was stirred at 60 °C for 16 h. The slurry was filtered through fritted discs and washed 10 times with toluene (10× 20 ml). The resultant solid was dried under vacuum at room temperature for 16 h. 2 ml of MAO was added to **1** (300 mg) in toluene (10 ml) contained in a flask provided with a mechanical agitator. The mixture was stirred for 1 h with a light red suspension being formed. Toluene was eliminated in vacuo and the resulting material was dried for 2 h at room temperature to give a pink-salmon free flowing solid.

2.2.2. MCM-41/[Zr{Me_2Si(η^5-C_5Me_4)(η^5-C_5H_4)}Cl_2]/MAO (**2**)

The modified mesoporous surface **2** was prepared following the procedure described for **1**, using MCM-41 (1.00 g) and [Zr{Me_2Si(η^5-C_5Me_4)(η^5-C_5H_4)}Cl_2] (44 mg, 0.11 mmol).

2.2.3. MCM-41/[Zr{Me_2Si(η^5-C_5Me_4)(η^5-$C_5H_3Bu^t$)}Cl_2]/MAO (**3**)

The modified mesoporous surface **3** was prepared following the procedure described for **1**, using MCM-41 (1.00 g) and [Zr{Me_2Si(η^5-C_5Me_4)(η^5-$C_5H_3Bu^t$)}Cl_2] (50 mg, 0.11 mmol).

2.2.4. SG/[Zr(η^5-C_5H_5)$_2$$Cl_2$]/MAO (**4**)

The modified surface **4** was prepared following the procedure described for **1**, using SG (1.00 g) and [Zr(η^5-C_5H_5)$_2$$Cl_2$] (32 mg, 0.11 mmol).

2.2.5. SG/[Zr{Me_2Si(η^5-C_5Me_4)(η^5-C_5H_4)}Cl_2]/MAO (**5**)

The modified surface **5** was prepared following the procedure described for **1**, using SG (1.00 g) and [Zr{Me_2Si(η^5-C_5Me_4)(η^5-C_5H_4)}Cl_2] (44 mg, 0.11 mmol).

2.2.6. SG/[Zr{Me_2Si(η^5-C_5Me_4)(η^5-$C_5H_3Bu^t$)}Cl_2]/MAO (**6**)

The modified surface **6** was prepared following the procedure described for **1**, using SG (1.00 g) and [Zr{Me_2Si(η^5-C_5Me_4)(η^5-$C_5H_3Bu^t$)}Cl_2] (50 mg, 0.11 mmol).

2.3. Characterization of the modified mesoporous surfaces

Infrared spectra were recorded on a Thermo-Nicolet Avatar 380 FT-IR spectrophotometer using an infrared cell equipped with CaF_2 or KBr windows; this set-up allowed in situ studies. A total of 32 scans were typically accumulated for each spectrum (resolution 2 cm^{-1}). The samples consisted of ca. 20 mg of silica pressed into a self-supported disc of 1 cm diameter. The samples were dried at 500 °C for 16 h. Zirconocene grafting was performed using a 10^{-2} M solution of the metallocene complex in toluene to give approximately 1% Zr/SiO_2. The samples were maintained at 60 °C for 1 h, washed with toluene and dried in vacuo at room temperature until no further change was observed (sublimation of the excess complex was observed). MAO was added as a 10% solution in toluene and the amount was calculated to give an Al/Zr ratio of ca. 1:100. After evaporation of solvent, the sample was exposed to ca. 2 bars of ethylene for 10 min and evacuated in vacuo. The FT-IR analysis was repeated on three different samples in order to ensure reproducibility. ^{13}C-CP and ^{29}Si MAS NMR spectra were recorded on a Varian-Infinity Plus spectrometer at 400 MHz operating at 100.52 MHz proton frequency (4 μs 90° pulse, 4000 transients, spinning speed of 6 MHz, contact time 3 ms, pulse delay 1.5 s). X-ray diffraction (XRD) pattern of the silicas was obtained on a Phillips diffractometer model PW3040/00 X'Pert MPD/MRD at 45 kV and 40 mA, using a wavelength Cu Kα (λ = 1.5418 Å). The zirconium content was determined by inductively coupled plasma-atomic emission spectroscopy (ICP-AES) using a Varian Vista AX model. The samples (0.1 g) were dissolved in aqueous hydrofluoric and sulphuric acid. After dissolved, the sample was heated to evaporate water and hydrofluoric acid and the sample was calcined to eliminate the organic material, and the residue was made up to 250 ml with Milli-Q water using a volumetric flask. A standard solution of Zr (1000 μg/ml in water) was used for the calibration curve. The thermal stability of the modified mesoporous silicas was studied using a Setsys 18 A (Setaram) thermogravimetric analyzer, using a platinum crucible of 100 μL. A synthetic air atmosphere was used and the temperature increased from 25 to 800 °C at a speed of 10 °C/min. N_2 gas adsorption–desorption isotherms were recorded using a Micromeritics TriStar 3000 analyzer. Polymer molecular weights and distributions were determined by gel permeation chromatography (GPC Waters 150C Plus) in 1,2,4-trichlorobenzene at 145 °C, using polystyrene as standard for calibration.

Scanning electron micrographs and morphological analysis were carried out on a XL30 ESEM Philips with an energy dispersive spectrometry system (EDS). The samples were treated with a sputtering method with the following parameters—sputter time: 100 s; sputter current: 30 mA; film thickness: 20 nm using a sputter coater BAL-TEC SCD 005. Conventional transmission electron microscopy (TEM) was carried out on a TECNAI 20 Philips electron microscope, operating at 200 kV.

2.4. Polymerization

The polymerization experiments were carried out in a 1-l glass reactor using toluene as a solvent (ca. 250 ml). Toluene (230 ml), TIBA (triisobutylaluminum) scavenger (2 ml) and the modified

mesoporous surface in freshly distilled toluene (20 ml) were introduced, in this order, into the reactor and thermostatized at 343 K. Nitrogen was removed and a continuous flow of ethylene (2 bar) was introduced for 15 min. The reaction was then quenched by the addition of acidified methanol. The polymer was collected, washed with methanol and acetone, and dried under vacuum at room temperature for 24 h.

3. Results and discussion

3.1. Preparation of the modified supports

Silica gel has been the most studied support whilst other silicas, e.g. mesoporous silicas such as MCM-41, have been receiving less attention. Nevertheless, examples of MCM-41 have been reported and include two main immobilization techniques: (i) direct anchoring of metallocene complex on the support and (ii) pretreatment of the support with alkylaluminum species or methyaluminoxane (MAO) followed by reaction with the metallocene compound. As far as the first method is concerned, Kageyama and his co-workers first synthesized crystalline linear polyethylene nano-fibres with MSF (mesoporous silica fibre) supported titanocene dichloride catalysts at ethylene pressure of 10 atm [16]. In 1996 Braca et al. [17] and in 1998 Michelloti et al. [18] reported that zeolites could be suitable supports due to the possibility of entrapping organometallic complexes in their pores. The pore size of the support has been shown to strongly influence catalytic activity, polymer molecular weight and stereoregularity. It is noteworthy to point out the work developed by Rahiala et al. in 1999, in which the effect of the structure and surface properties of different supports employed (commercial Grace silica, MCM-41, and aluminum-modified MCM-41) on metallocene adsorption ([Zr(η^5-C_5H_5)$_2$Cl$_2$]) and catalyst activity in ethylene polymerization were studied [19]. More examples include preparation of syndiotactic polypropylene [20] and nano-polyethylene fibres [21] through extrusion polymerization using the mesopores of the support. Finally, Silveria et al. reported the effect of grafting two different metallocene complexes on the same support at different orders and molecular ratios, on catalytic activity and polymer properties [22]. Concerning the second method, the use of a well-defined mesoporous MCM-41/MAO system as catalyst carrier has been shown to be the most successful in polymerization reactions in terms of productivity and polymer properties. Kaminsky et al. [20], Van Looveren et al. [23] and Tudor and O'Hare [24] presented systems based on the use of a pre-treated MCM-41 with MAO as promising heterogeneous catalysts in synthesizing syndiotactic polypropylene, co-oligomer of ethylene and propylene, and isotactic polypropylene, respectively.

MCM-41 used in the present study was dried at 773 K. The immobilization technique of direct anchoring of the metallocene complex on the support has been employed. The modified mesoporous surfaces have been extensively characterized and a comparative study in ethylene polymerization has been carried out.

A first modification of the surfaces under study was made by the grafting of an *ansa*-metallocene compound ([Zr{Me_2Si(η^5-C_5Me_4)(η^5-C_5H_4)}Cl$_2$] and [Zr{Me_2Si(η^5-C_5Me_4)(η^5-$C_5H_3Bu^t$)}Cl$_2$], taking as reference the non-*ansa*-metallocene [Zr(η^5-C_5H_5)$_2$Cl$_2$]). This first modification, at mild temperatures, led to a reaction between one of the chlorine atoms of the corresponding metallocene complex, not only with the acidic silanol groups but also with the reactive siloxane bridges, giving rise to μ-oxo surface species [12a,b]. A second modification was made after contact with MAO to give MCM-41/metallocene/MAO (metallocene = [Zr(η^5-C_5H_5)$_2$Cl$_2$] (**1**), [Zr{Me_2Si(η^5-C_5Me_4)(η^5-C_5H_4)}Cl$_2$] (**2**) and [Zr{Me_2Si(η^5-C_5Me_4)(η^5-$C_5H_3Bu^t$)}Cl$_2$] (**3**)). The cationic species generated at the surface, by the action of MAO, contain potentially active sites in the polymerization of α-olefins (Scheme 1). The ion pair is completed by the supported anionic [MAO-Me]$^-$ fragment, which can be easily displaced from the zirconium coordination sphere to allow entry of the monomer in the polymerization process.

For comparative reasons, the effect of a different and well-known support such as silica gel has been included in this study. Metallocene complexes were supported on silica gel in an identical manner to that employed for the mesoporous surfaces to give the heterogeneous catalytic systems SG/metallocene/MAO (metallocene = [Zr(η^5-C_5H_5)$_2$Cl$_2$] (**4**), [Zr{Me_2Si(η^5-C_5Me_4)(η^5-C_5H_4)}Cl$_2$] (**5**) and [Zr{Me_2Si(η^5-C_5Me_4)(η^5-$C_5H_3Bu^t$)}Cl$_2$] (**6**)).

With the objective of determining the maximum loading of zirconium on the MCM-41 surface, the quantity of zirconium contained in the initial solutions of [Zr{Me_2Si(η^5-C_5Me_4)(η^5-C_5H_4)}Cl$_2$] in toluene was varied (Table 1). The zirconium loading approaches a saturation limit, near to 1.6%, which is in agreement with previously reported results [19]. However, this limit is very low (a superior theoretical maximum loading is expected) and was not improved even when a large excess of metallocene complexes and long reaction times were used. The weak basicity of the chloro ligands and the weak acidity of the Si–OH groups may explain the difficulty in obtaining higher loadings.

Table 2 reports the grafted metal content determined for the different supported systems resulting from the immobilization of [Zr(η^5-C_5H_5)$_2$Cl$_2$], [Zr{Me_2Si(η^5-C_5Me_4)(η^5-C_5H_4)}Cl$_2$] and [Zr{Me_2Si(η^5-C_5Me_4)(η^5-$C_5H_3Bu^t$)}Cl$_2$] on MCM-41 and SG. According to the results presented in Table 2, the Zr/SiO_2 wt.% lies between 0.33 and 0.69. In the particular case of MCM-41 at 60 °C percentages between 0.33 and 0.38 were observed. These values are close to those reported in the literature on supports submitted to thermal activation before the grafting of the metallocene: 0.3 and

Table 1
%Zr grafted onto the silica support (MCM-41/[Zr{Me_2Si(η^5-C_5Me_4)(η^5-C_5H_4)}Cl$_2$]).

Zr_0 (wt.%)[a]	Zr_{exp} (wt.%)[b]
1	0.33
1.5	0.78
2	1.6
3	1.6

[a] Theoretical Zr (wt.%).
[b] Experimental Zr (wt.%).

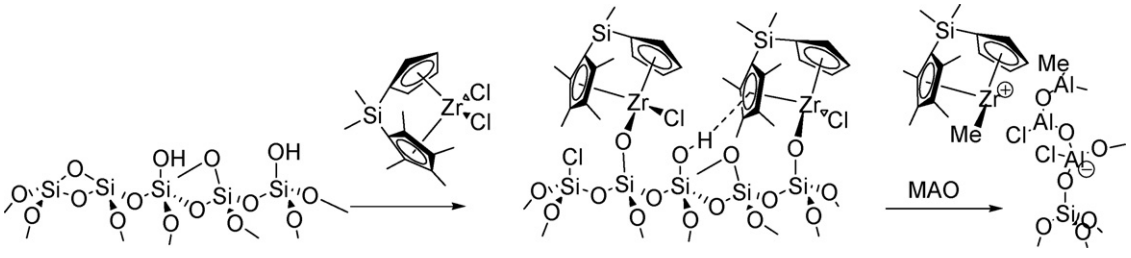

Scheme 1.

Table 2
%Zr grafted on the silica support.

Catalyst	Zr_0 (wt.%)[a]	Zr_{exp} (wt.%)[b]
MCM-41/[Zr(η^5-C_5H_5)$_2$$Cl_2$]	1	0.38
MCM-41/[Zr{Me_2Si(η^5-C_5Me_4)(η^5-C_5H_4)}Cl_2]	1	0.33
MCM-41/[Zr{Me_2Si(η^5-C_5Me_4)(η^5-$C_5H_3Bu^t$)}Cl_2]	1	0.34
SG/[Zr(η^5-C_5H_5)$_2$$Cl_2$]	1	0.69
SG/[Zr{Me_2Si(η^5-C_5Me_4)(η^5-C_5H_4)}Cl_2]	1	0.56
SG/[Zr{Me_2Si(η^5-C_5Me_4)(η^5-$C_5H_3Bu^t$)}Cl_2]	1	0.54

[a] Theoretical Zr (wt.%).
[b] Experimental Zr (wt.%).

0.38 Zr/SiO_2 wt.% [25]. However, a ratio close to 0.60% was found for the SG. MCM-41 has cavities with connecting channels of specific dimensions. Unlike SG, this support possesses hexagonal pore structures. The metallocene complex is thought to be able to penetrate the pores of the MCM-41 and reside inside, but it can also be a restriction for its grafting.

3.2. Characterization of the modified MCM-41 supports

An extensive characterization of the new materials has been carried out. The modified MCM-41 systems, MCM-41/[Zr{Me_2Si(η^5-C_5Me_4)(η^5-C_5H_4)}Cl_2] and MCM-41/[Zr{Me_2Si(η^5-C_5Me_4)(η^5-C_5H_4)}Cl_2]/MAO were chosen as representative examples.

MAS NMR spectroscopy has proven to be a useful tool in monitoring surface reactions of organometallic reagents [26]. The ^{13}C-CP MAS NMR study proved that the metallocene is bound to the support surface. The ^{13}C-CP MAS NMR spectrum of MCM-41/[Zr{Me_2Si(η^5-C_5Me_4)(η^5-C_5H_4)}Cl_2] is presented in Fig. 1a and shows four signals at −0.4, 12.2, 111.3 and 131.1 ppm. The signals at 111.3 and 131.1 ppm were assigned to the carbon atoms of the C_5 rings (C_5H_4 and C_5Me_4, respectively). A signal was observed at 12.2 ppm corresponding to the carbon atoms of the methyl groups of the C_5Me_4 moiety. Finally, the peak at −0.4 ppm refers to the carbon atoms of the $SiMe_2$ group.

After modification with MAO (Fig. 1b), a broad signal was observed at 0.7 ppm and assigned to Si–CH_3 and Al–CH_3 moieties. The signal broadening of the latter ^{13}C resonance probably arose not only from differently composed Al–CH_3 surface species but also by quadrupolar interactions with the directly attached aluminum (^{27}Al, I = 5/2) [27]. A signal was observed at 29 ppm corresponding to the carbon atoms of the methyl group of the C_5Me_4 moiety. The signals corresponding to the carbon atoms of the methyl groups (Zr–Me and $SiMe_2$) are most likely hidden under the peak at 0.7 ppm. Carbon atoms of the C_5 rings gave signals at 132 and 137 ppm.

Air-exposure of the sample, MCM-41/[Zr{Me_2Si(η^5-C_5Me_4)(η^5-C_5H_4)}Cl_2]/MAO, indicated a possible degradation product. The complete disappearance of the Al–CH_3 signal and the retention of the Si–CH_3 were observed. In addition, a broad resonance at approximately 58 ppm, attributable to Si–OCH_3 moiety, was clearly visible (Fig. 1c).

For MCM-41/[Zr{Me_2Si(η^5-C_5Me_4)(η^5-C_5H_4)}Cl_2] and MCM-41/[Zr{Me_2Si(η^5-C_5Me_4)(η^5-C_5H_4)}Cl_2]/MAO the fate of the silanol groups was followed by ^{29}Si MAS NMR (Fig. 2). Fig. 2a reveals Si atoms with hydroxyl bound groups, such as [$Si(OSi)_2(OH)_2$] (Q_2, δ = −91.6), [$Si(OSi)_2(OH)$] (Q_3, δ = −100.6) and [$Si(OSi)_2$] (Q_4, δ = −110). After grafting the metallocene complex, no remarkable modification of the Q_n (n = 2, 3, 4) sites was observed, although a new band appeared at −62 ppm corresponding to a T site (Fig. 2b). The disappearance of Q_2 and Q_3 resonances and also the observation of a band at −62 ppm after treatment with MAO clearly

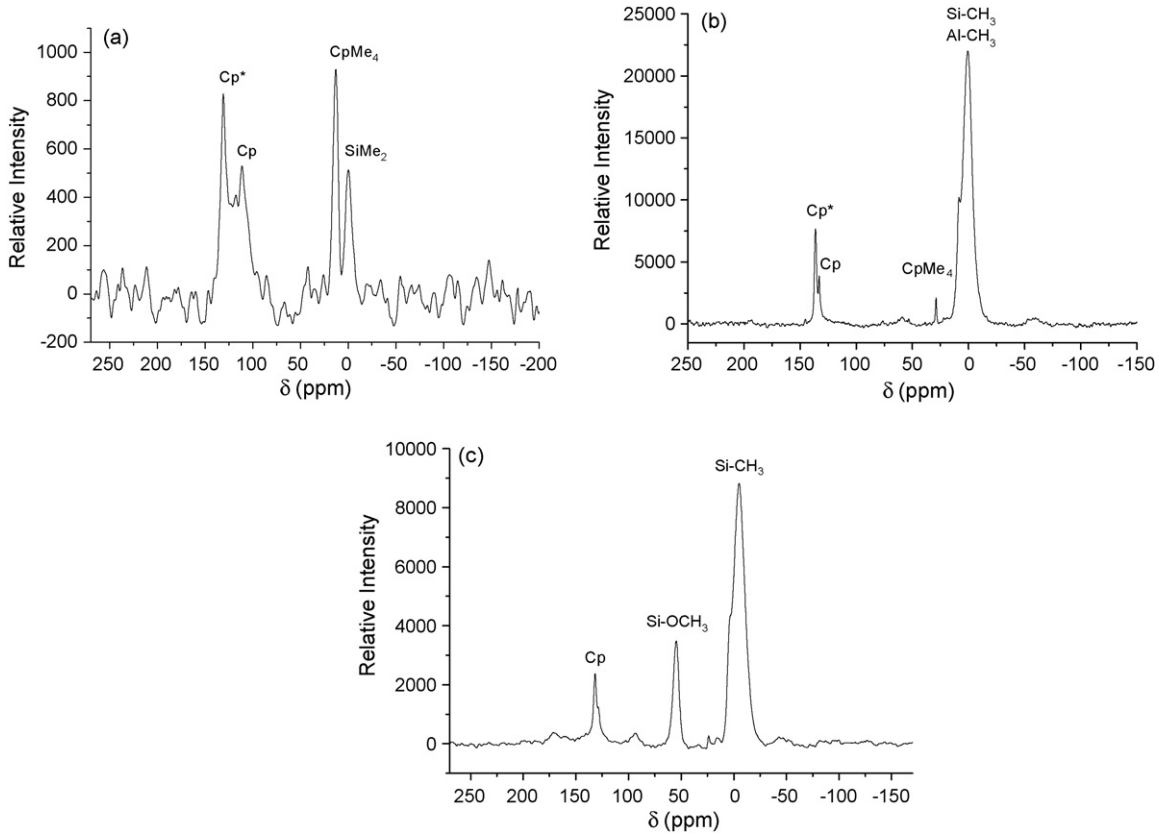

Fig. 1. ^{13}C-CP MAS NMR spectra: (a) MCM-41/[Zr{Me_2Si(η^5-C_5Me_4)(η^5-C_5H_4)}Cl_2], (b) MCM-41/[Zr{Me_2Si(η^5-C_5Me_4)(η^5-C_5H_4)}Cl_2]/MAO and (c) air-exposed MCM-41/[Zr{Me_2Si(η^5-C_5Me_4)(η^5-C_5H_4)}Cl_2]/MAO.

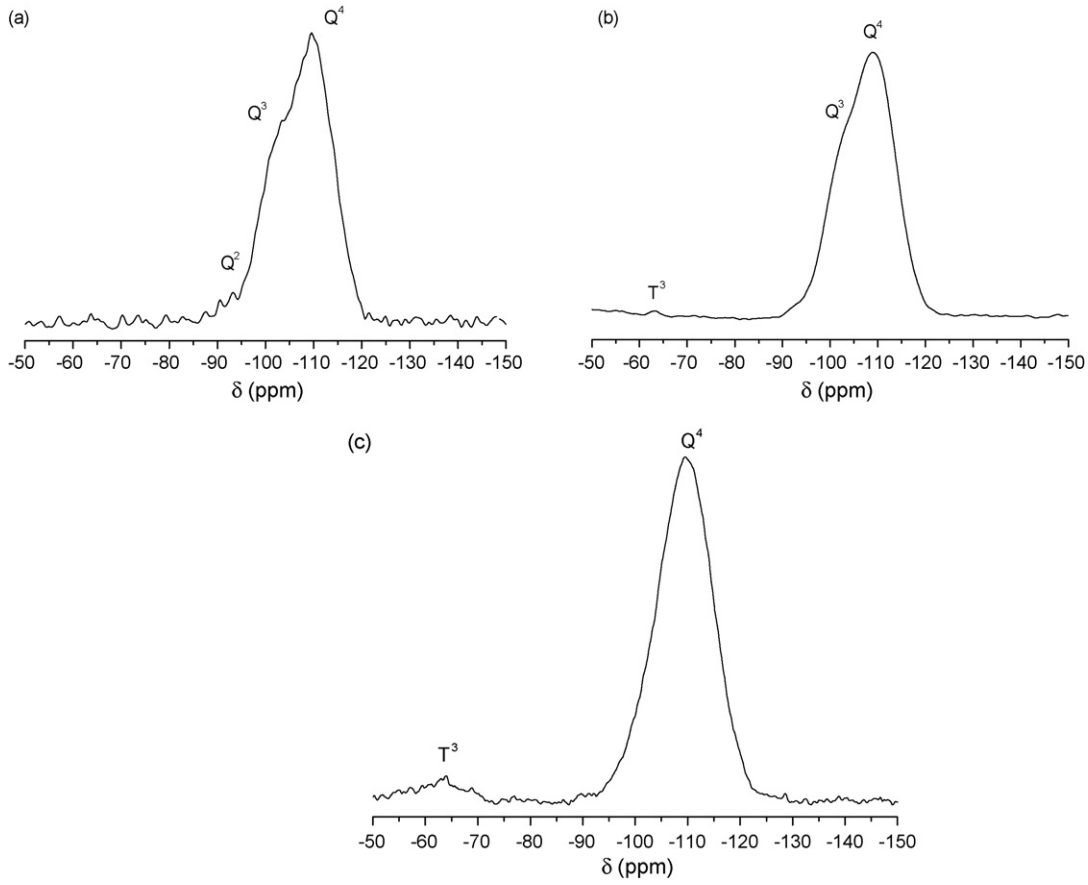

Fig. 2. ^{29}Si MAS NMR spectra: (a) MCM-41, (b) MCM-41/[Zr{$Me_2Si(\eta^5$-$C_5Me_4)(\eta^5$-$C_5H_4)$}Cl_2] and (c) MCM-41/[Zr{$Me_2Si(\eta^5$-$C_5Me_4)(\eta^5$-$C_5H_4)$}Cl_2]/MAO.

demonstrate the covalent bonding of the MAO to the silanol groups of the MCM-41 (Fig. 2c).

3.3. Structural features of the modified MCM-41 support

The morphologies of the commercial SG and MCM-41 are clearly different. The main structural feature of MCM-41 gives rise to XRD reflections which are typical of hexagonally ordered mesoporous material [28]. Fig. 3a shows the XRD pattern of MCM-41. The characteristic Bragg peaks with *d*-spacing 39.31, 22.74 and 18.97 Å correspond to reflections from the (1 0 0), (1 1 0), and (2 0 0) planes, respectively (Table 3).

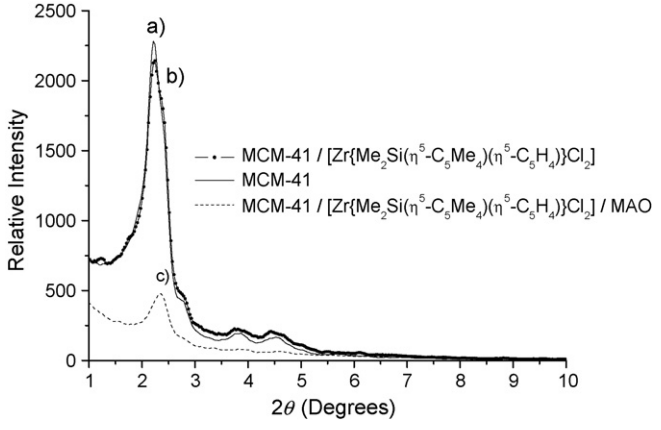

Fig. 3. Powder low-angle XRD patterns of: (a) MCM-41, (b) MCM-41/[Zr{$Me_2Si(\eta^5$-$C_5Me_4)(\eta^5$-$C_5H_4)$}Cl_2] and (c) MCM-41/[Zr{$Me_2Si(\eta^5$-$C_5Me_4)(\eta^5$-$C_5H_4)$}Cl_2]/MAO.

No remarkable alterations were observed in the XRD pattern after the grafting of the metallocene complex. MCM-41/[Zr{$Me_2Si(\eta^5$-$C_5Me_4)(\eta^5$-$C_5H_4)$}Cl_2] displayed a well-resolved pattern at low 2θ with a very sharp (1 0 0) diffraction peak at 2.25° and two weak peaks (1 1 0 and 2 0 0) at 3.91° and 4.59°, respectively (Fig. 3b, Table 3). These can be indexed as a hexagonal lattice with *d*-spacing values of 39.1, 22.6 and 19.3 Å, respectively. A unit cell parameter, a_0, of 45.15 Å was obtained [28].

The XRD structural analysis of MCM-41/[Zr{$Me_2Si(\eta^5$-$C_5Me_4)(\eta^5$-$C_5H_4)$}Cl_2]/MAO showed that the hexagonal pore structure of MCM-41 becomes less ordered after modification with MAO. However, the XRD pattern suggests the maintenance of the structural order of the synthesized materials after modification.

Fig. 4a shows the thermogravimetric analysis curve of MCM-41/[Zr{$Me_2Si(\eta^5$-$C_5Me_4)(\eta^5$-$C_5H_4)$}Cl_2]. Water and organic material were released or burned from the structure in three main steps (i) removal of water inside the pores (90–200 °C), (ii) desorption of the main part of the template molecules and the combustion of

Table 3
XRD data of the MCM-41, MCM-41/[Zr{$Me_2Si(\eta^5$-$C_5Me_4)(\eta^5$-$C_5H_4)$}Cl_2] and MCM-41/[Zr{$Me_2Si(\eta^5$-$C_5Me_4)(\eta^5$-$C_5H_4)$}Cl_2]/MAO.

Material	(*h k l*)	2θ (°)	*d*-Spacing (Å)
MCM-41	1 0 0	2.24	39.31
	1 1 0	3.88	22.74
	2 0 0	4.65	18.97
MCM-41/[Zr{$Me_2Si(\eta^5$-$C_5Me_4)(\eta^5$-$C_5H_4)$}Cl_2]	1 0 0	2.26	39.10
	1 1 0	3.91	22.59
	2 0 0	4.59	19.25
MCM-41/[Zr{$Me_2Si(\eta^5$-$C_5Me_4)(\eta^5$-$C_5H_4)$}Cl_2]/MAO	1 0 0	2.36	37.35

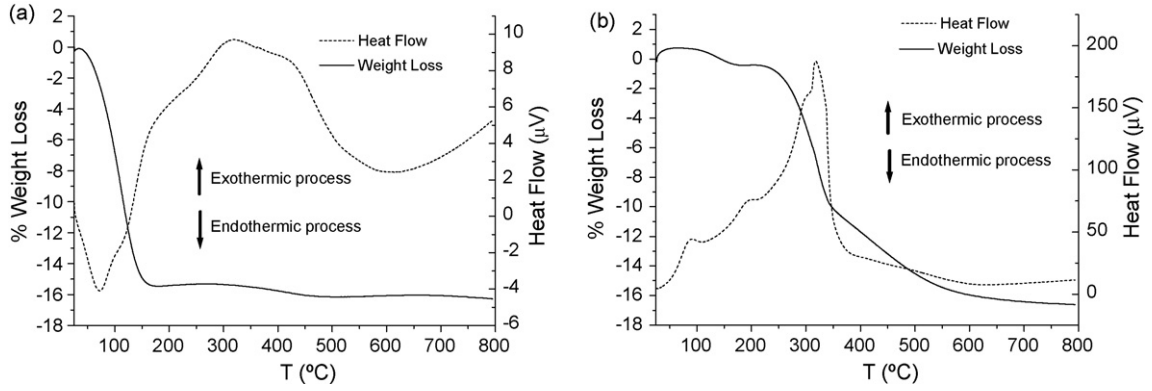

Fig. 4. Thermogravimetric and heat flow curves: (a) MCM-41/[Zr{$Me_2Si(\eta^5$-$C_5Me_4)(\eta^5$-$C_5H_4)$}Cl_2] and (b) MCM-41/[Zr{$Me_2Si(\eta^5$-$C_5Me_4)(\eta^5$-$C_5H_4)$}Cl_2]/MAO.

the remaining carbon species (200–340 °C), and (iii) loss of water released as a result of condensation of silanol groups to siloxane fragments (>350 °C). After modification with MAO (Fig. 4b) all the organic material was burned off and no dealumination seemed to occur during the calcinations. According to the literature partial dealumination has been observed at calcination temperatures higher than 400 °C [29].

The determination of nitrogen adsorption/desorption isotherms is an efficient tool to characterize the nature of porous host systems. Mesoporous materials of the type MCM-41, MCM-41/[Zr{$Me_2Si(\eta^5$-$C_5Me_4)(\eta^5$-$C_5H_4)$}Cl_2] and MCM-41/[Zr{$Me_2Si(\eta^5$-$C_5Me_4)(\eta^5$-$C_5H_4)$}Cl_2]/MAO display type-IV isotherms according to the IUPAC nomenclature [30], which are characterized by a sharp inflection point due to capillary condensation (Fig. 5). In the case of MCM-41 and MCM-41/[Zr{$Me_2Si(\eta^5$-$C_5Me_4)(\eta^5$-$C_5H_4)$}Cl_2] an H1 hysteresis loop, that is representative of mesoporous surfaces, was observed. The effective mean pore diameters of MCM-41 and MCM-41/[Zr{$Me_2Si(\eta^5$-$C_5Me_4)(\eta^5$-$C_5H_4)$}Cl_2] were estimated at 36 and 35 Å, respectively (Table 4). The volume adsorbed for MCM-41 and MCM-41/[Zr{$Me_2Si(\eta^5$-$C_5Me_4)(\eta^5$-$C_5H_4)$}Cl_2] isotherms sharply increased at a relative pressure (P/P_0) of approximately 0.3, representing capillary condensation of nitrogen within the uniform mesoporous structure. The inflection position shifted slightly towards lower relative pressures and the volume of nitrogen adsorbed decreased with the modification in the case of MCM-41/[Zr{$Me_2Si(\eta^5$-$C_5Me_4)(\eta^5$-$C_5H_4)$}Cl_2]. Exposure of the material MCM-41/[Zr{$Me_2Si(\eta^5$-$C_5Me_4)(\eta^5$-$C_5H_4)$}Cl_2] to MAO resulted in N_2 adsorption/desorption isotherms that shows the filling of the mesopores (pore diameter of 25 Å) (Fig. 5c). Capillary condensation within the pores of the MCM-41/[Zr{$Me_2Si(\eta^5$-$C_5Me_4)(\eta^5$-$C_5H_4)$}Cl_2]/MAO disappears, which illustrates that the uniform pores are narrowed from mesoporous to microporous dimensions.

Table 4 shows the physical parameters obtained from nitrogen isotherms, such as the BET surface area (S_{BET}), (BJH) average pore diameter and wall thickness for (a) MCM-41, (b) MCM-41/[Zr{$Me_2Si(\eta^5$-$C_5Me_4)(\eta^5$-$C_5H_4)$}Cl_2] and (c) MCM-41/[Zr{$Me_2Si(\eta^5$-$C_5Me_4)(\eta^5$-$C_5H_4)$}Cl_2]/MAO. As expected, the pores become slightly smaller as a result of immobilization of the *ansa*-zirconocene dichloride. The incorporation of molecules inside the pores of the MCM-41 is justified through the increase in wall thickness (calculated data in Table 4).

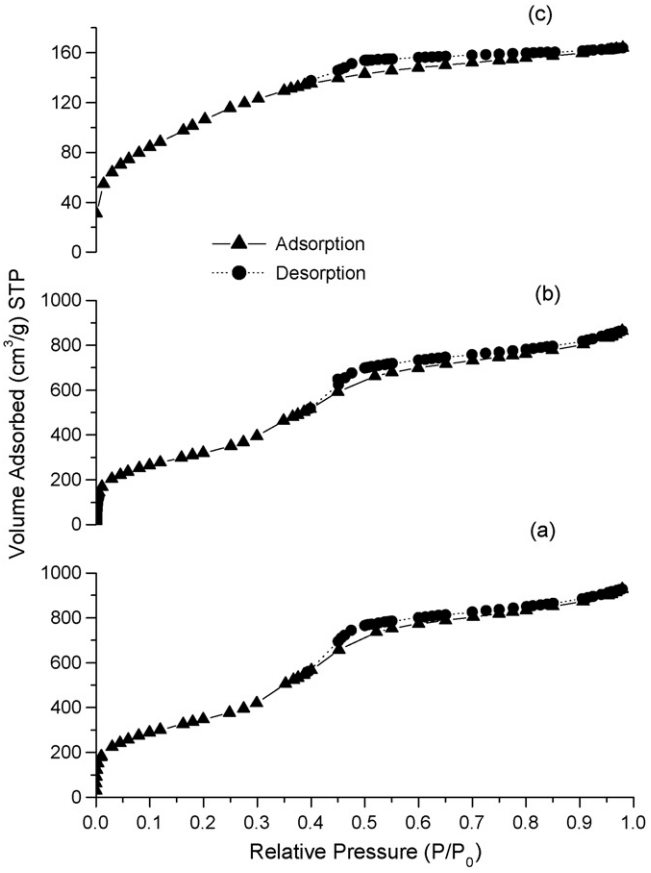

Fig. 5. Nitrogen adsorption/desorption isotherms: (a) MCM-41, (b) MCM-41/[Zr{$Me_2Si(\eta^5$-$C_5Me_4)(\eta^5$-$C_5H_4)$}Cl_2] and (c) MCM-41/[Zr{$Me_2Si(\eta^5$-$C_5Me_4)(\eta^5$-$C_5H_4)$}Cl_2]/MAO.

The maximum Van der Waals radius of the *ansa*-zirconocene dichloride molecule is approximately 6 Å. The pores, with an

Table 4
Physical parameters of MCM-41, MCM-41/[Zr{$Me_2Si(\eta^5$-$C_5Me_4)(\eta^5$-$C_5H_4)$}Cl_2] and MCM-41/[Zr{$Me_2Si(\eta^5$-$C_5Me_4)(\eta^5$-$C_5H_4)$}Cl_2]/MAO measured by N_2 adsorption–desorption isotherms.

Sample	BET surface area (m^2/g)	Total pore volume (cm^3/g)	Pore diameter (BJH)[a] (Å)	Wall thickness (Å)
MCM-41	1240	1.42	36	9.4
MCM-41/[Zr{$Me_2Si(\eta^5$-$C_5Me_4)(\eta^5$-$C_5H_4)$}Cl_2]	1145	1.32	35	10.1
MCM-41/[Zr{$Me_2Si(\eta^5$-$C_5Me_4)(\eta^5$-$C_5H_4)$}Cl_2]/MAO	400	0.25	25	18.1

[a] Barrett, Joyner and Halenda.

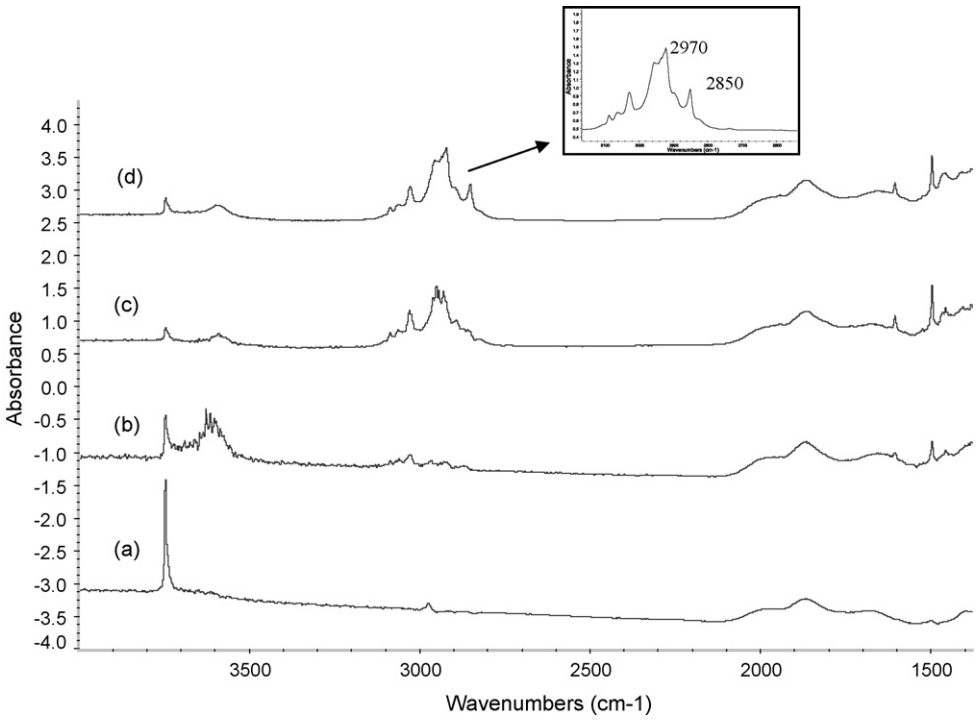

Fig. 6. FT-IR spectra: (a) MCM-41, (b) MCM-41/[Zr{$Me_2Si(\eta^5$-$C_5Me_4)(\eta^5$-$C_5H_4)$}Cl_2], (c) MCM-41/[Zr{$Me_2Si(\eta^5$-$C_5Me_4)(\eta^5$-$C_5H_4)$}Cl_2]/MAO and (d) after contact with C_2H_4.

average diameter of 36 Å for MCM-41, would therefore provide more than enough space for the metallocene molecule to bind to the surface OH groups inside the cavities. The wall thickness for MCM-41, MCM-41/[Zr{$Me_2Si(\eta^5$-$C_5Me_4)(\eta^5$-$C_5H_4)$}Cl_2] and MCM-41/[Zr{$Me_2Si(\eta^5$-$C_5Me_4)(\eta^5$-$C_5H_4)$}Cl_2]/MAO (9.4, 10.1 and 18.1 Å, respectively) was calculated using the following equation [31]:

$$\text{Wall thickness} = \frac{2d_{100}}{\sqrt{3}} - \text{BJH average pore diameter}$$

3.4. Activity in ethylene polymerization of polymers properties

A preliminary FT-IR "in situ" study of the heterogeneization of [Zr{$Me_2Si(\eta^5$-$C_5Me_4)(\eta^5$-$C_5H_4)$}Cl_2] and its subsequent application as a catalyst in ethylene polymerization is shown in Fig. 6. The spectrum of MCM-41 preheated at 773 K has a sharp band at 3745 cm^{-1} (assigned to isolated OH groups) [32] with a broad shoulder at 3671 cm^{-1}, which can be attributed to silanol groups that are perturbed due to interparticle contacts [32] or to OH groups retained deep within the pores [33] (Fig. 6a). Bands at 1866 and 1640 cm^{-1} are combinations and overtone bands of Si–O network bonds. After contact with the metallocene solution and removal of the solvent (Fig. 6b), new bands appeared in the 2900 and 1400 cm^{-1} regions and these correspond to stretching and bending modes of the cyclopentadienyl ligands. The OH groups that were initially isolated are now partially perturbed, generating broad ν(OH) bands at lower frequencies due to an interaction with the cyclopentadienyl π-electron system through hydrogen bonding [34]. The IR spectrum of a sample of MCM-41/[Zr{$Me_2Si(\eta^5$-$C_5Me_4)(\eta^5$-$C_5H_4)$}Cl_2] treated with MAO (approx. Al/Zr = 100) is shown in Fig. 6c. After this treatment, the infrared band attributed to isolated silanol groups (at 3747 cm^{-1}) disappeared almost completely at room temperature, indicating a reaction between basic methyl groups of MAO and the acidic silanol groups. At the same time, new bands appeared in the ν(CH) region; one strong band at 2940 cm^{-1} and three weak bands at 2898, 2856 and 2838 cm^{-1}. These bands have been assigned to stretching vibrations of C–H bonds of the methyl groups in MAO. This situation could lead to the formation of the potentially active alkyl cationic surface species (Scheme 1). The activity of MCM-41/[Zr{$Me_2Si(\eta^5$-$C_5Me_4)(\eta^5$-$C_5H_4)$}Cl_2]/MAO in ethylene polymerization was confirmed by following the appearance of small vibrations due to polyethylene in the regions 3000–2800 cm^{-1}. Bands were observed at 2970 and 2850 cm^{-1}, which correspond to the ν(CH) vibrations of polyethylene and demonstrate the beginning of the polymerization reaction (Fig. 6d).

The modified mesoporous surfaces MCM-41/metallocene/MAO (metallocene = [$Zr(\eta^5$-$C_5H_5)_2Cl_2$] (**1**), [Zr{$Me_2Si(\eta^5$-$C_5Me_4)(\eta^5$-$C_5H_4)$}Cl_2] (**2**) and [Zr{$Me_2Si(\eta^5$-$C_5Me_4)(\eta^5$-$C_5H_3Bu^t)$}Cl_2] (**3**)) are presented as heterogeneous catalysts in the polymerization of ethylene. For comparative reasons, the systems SG/metallocene/MAO (metallocene = [$Zr(\eta^5$-$C_5H_5)_2Cl_2$] (**4**), [Zr{$Me_2Si(\eta^5$-$C_5Me_4)(\eta^5$-$C_5H_4)$}Cl_2] (**5**) and [Zr{$Me_2Si(\eta^5$-$C_5Me_4)(\eta^5$-$C_5H_3Bu^t)$}Cl_2] (**6**)) were also studied.

For MCM-41 systems the *ansa*-metallocene catalyst presented comparable activity in polymerization to their non-*ansa* analogue. Among the two supported catalyst systems examined, MCM-41/metallocene/MAO **1**–**3** catalysts were found to be less active in the polymerization of ethylene (Table 5). However, it is well-known that the higher accessible surface area for the metallocene catalyst in the MCM-41 to that in the SG, reduces the possibility of deactivation by binuclear complex formation, which has been reported as the most probable way of forming inactive sites after immobilization [10]. Alternatively, the lower activity might be due to the steric hindrance encountered in the MCM-41 pores which restricts the diffusion of the monomer inside the cavities.

Table 5 shows the catalytic activity of the modified surfaces **1**–**6**, polymer molecular weight, polymer molecular weight distribution and polymer melting point. An increase in polymer molecular weight for the MCM-41 systems, in comparison with the SG systems was observed, and attributed to a reduction in the rate of chain transfer due to the steric constraints of the mesoporous surface pores. The polydispersity of all the polymers gave a value of

Table 5
Ethylene polymerization results for **1**–**6**.

Catalyst	Activity (kgPE/(molZr h bar))	M_w (g/mol)	M_n/M_w	T_m (°C)
MCM-41/[Zr(η^5-C_5H_5)$_2$$Cl_2$]/MAO (**1**)	1228	285,000	3.0	134
MCM-41/[Zr{Me_2Si(η^5-C_5Me_4)(η^5-C_5H_4)}Cl_2]/MAO (**2**)	1400	276,000	2.9	133
MCM-41/[Zr{Me_2Si(η^5-C_5Me_4)(η^5-$C_5H_3Bu^t$)}Cl_2]/MAO (**3**)	1066	286,000	2.9	134
SG/[Zr(η^5-C_5H_5)$_2$$Cl_2$]/MAO (**4**)	1713	132,000	2.9	133
SG/[Zr{Me_2Si(η^5-C_5Me_4)(η^5-C_5H_4)}Cl_2]/MAO (**5**)	2239	158,000	2.9	134
SG/[Zr{Me_2Si(η^5-C_5Me_4)(η^5-$C_5H_3Bu^t$)}Cl_2]/MAO (**6**)	1818	172,000	2.8	134

Polymerization conditions: 70 °C, 2 bar monomer pressure, 300 mg of catalyst, 250 ml toluene, t_{pol} = 15 min.

approximately 3, suggesting some heterogeneity in the nature of the active sites, although this may also be due to other factors such as monomer concentration and/or temperature. All the catalysts produced polymers with melting points of around 134 °C, indicating the formation of linear high-density polyethylene [35]. This linear nature of the polymer was confirmed by ^{13}C NMR spectroscopy analysis of the polyethylene samples which showed essentially no branching. The activity values for the metallocene catalyst obtained in homogeneous conditions (*polymerization conditions*: 70 °C, 2 bar monomer pressure, 6 μmol of catalyst, 250 ml toluene, t_{pol} = 15 min) were found to be around 20 times higher than those obtained in analogous heterogeneous systems. The homogeneous catalytic system produced polyethylene with molecular weights of around 100,000 g/mol and polydispersities of 3. Heterogeneous catalysts normally produce polymers with higher molecular weight than those obtained with homogeneous catalysts [36]. This behaviour has already been observed and attributed to blocking of one of the sides of the polymerization active sites by the support, which hinders the deactivation step [37].

The ability to polymerize an olefin within the mesopores of an MCM-41 has been widely studied [38] and questioned [39]. The comparison of catalytic activity reported in the literature is rather difficult because of the different polymerization conditions used. The activities of the supported catalysts in the present study are high compared to the values obtained by other research groups using SiO_2/[Zr(η^5-C_5H_5)$_2$$Cl_2$] catalysts, where the active component was deposited directly on the support. Sacchi et al. obtained activities of 11–207 kgPE/(molZr h bar) at an Al/Zr ratio of 200–500 [36]. Rahiala et al. presented activities of 6100 kgPE/(molZr h bar) for the system MCM-41/[Zr(η^5-C_5H_5)$_2$$Cl_2$] but at an Al/Zr ratio of 2000 [19]. In all these cases the Al/Zr ratios used for the polymerization was higher than that used in this study.

In 2001, Lee et al. reported that [Zr(η^5-C_5H_5)$_2$$Cl_2$] supported directly on MCM-41 did not show any activity in ethylene polymerization [40]. The MAO-pretreatment of the SiO_2 support has usually been found to increase slightly the catalytic activity [41]. Tudor and O'Hare [24], Kaminsky et al. [20] and Ko et al. [42] have all presented heterogeneous catalytic systems based on MCM-41, previously modified by MAO, with subsequent grafting of prochiral alkene polymerization catalysts. Van Looveren et al. have reported the use of MCM-41/MAO as support in co-oligomerization with different catalysts [23].

3.5. Catalyst and polymers morphologies

The morphology of the polymer particle depends strongly on the shape and structure of the support employed. During early stages of polymerization the polymer forms a thin layer around the particle, which continues growing into the marginal areas of the support. Finally, the polymer grows from outside to inside and continues by a slow fragmentation of the support, allowing the access to new active centres and proceeding until the whole support is fragmented (replica phenomenon) [43].

Scanning electron microscopy (SEM) images of MCM-41 and MCM-41/[Zr{Me_2Si(η^5-C_5Me_4)(η^5-C_5H_4)}Cl_2]/MAO as well as the resulting polyethylene are shown in Fig. 7. Although slight differences in catalytic activity have been observed between *ansa* and non-*ansa*-metallocene complexes, no important deviations were noted in the catalyst and polymer morphologies. Fig. 7a shows a scanning electron microscope picture of the MCM-41. The MCM-41 particles are flat and have a hexagonal-to-round shape resulting in disk-like morphology. In addition, it is evident from the micrograph that the particles have a uniform size. The MCM-41 has an average particle diameter of 1.04 μm. No remarkable differences were found when the MCM-41 was modified by the grafting of the metallocene complex and the subsequent alteration by MAO (average particle diameter of 1.10 μm). According to Fig. 7b, the morphology of the support is maintained after catalyst preparation. The polyethylene obtained using the modified MCM-41 grew as shapeless aggregates. This may be due to poor dispersion of the catalyst in the mesoporous surface. On the other hand, the morphology of the polymer obtained from MCM-41/[Zr{Me_2Si(η^5-C_5Me_4)(η^5-C_5H_4)}Cl_2]/MAO followed the so-called replica phenomenon, where the catalysts were broken into small pieces, and the polymer resembles the broken catalyst particles (Fig. 7c). The catalyst produced particles of approximate diameter of 10 μm.

The mesostructure ordering and symmetry of MCM-41/[Zr{Me_2Si(η^5-C_5Me_4)(η^5-C_5H_4)}Cl_2] inferred from the XRD data was confirmed by the TEM images shown in Fig. 8a. The two-dimensional p6mm hexagonal symmetry can be clearly observed on the sample. An important modification of the surface and the pore distribution after treatment with MAO is clearly observed. A loss of periodicity of the MCM-41 material can be explained due to a partial blockage of the pores by the presence of MAO (Fig. 8b).

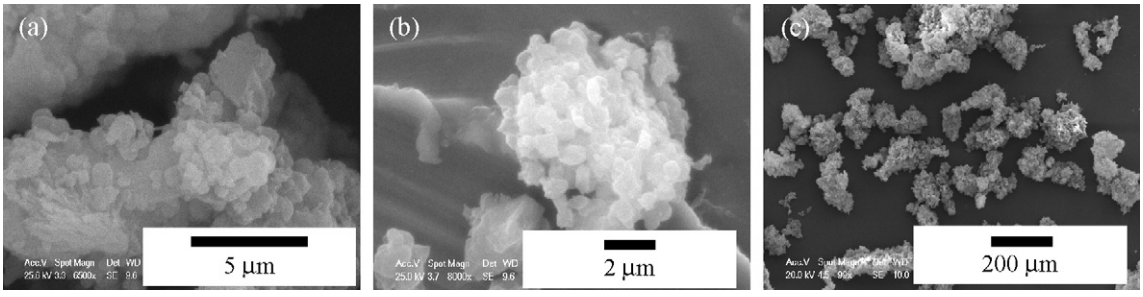

Fig. 7. Scanning electron microscope pictures: (a) MCM-41, (b) MCM-41/[Zr{Me_2Si(η^5-C_5Me_4)(η^5-C_5H_4)}Cl_2]/MAO and (c) polyethylene.

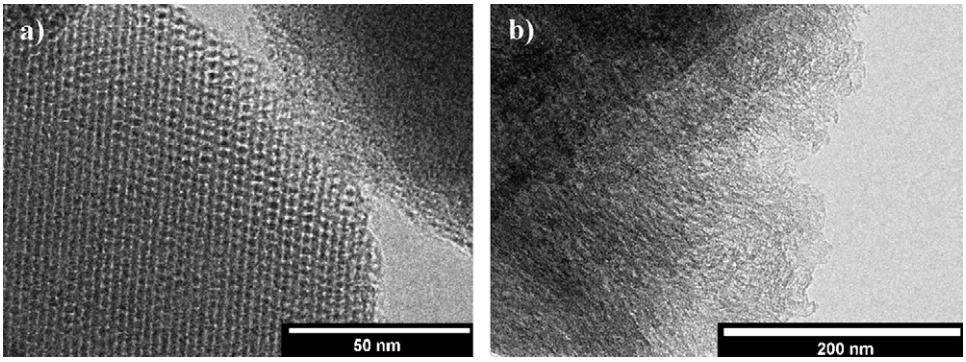

Fig. 8. Transmission electron microscope pictures: (a) MCM-41/[Zr{$Me_2Si(\eta^5$-$C_5Me_4)(\eta^5$-$C_5H_4)$}Cl_2] and (b) MCM-41/[Zr{$Me_2Si(\eta^5$-$C_5Me_4)(\eta^5$-$C_5H_4)$}Cl_2]/MAO.

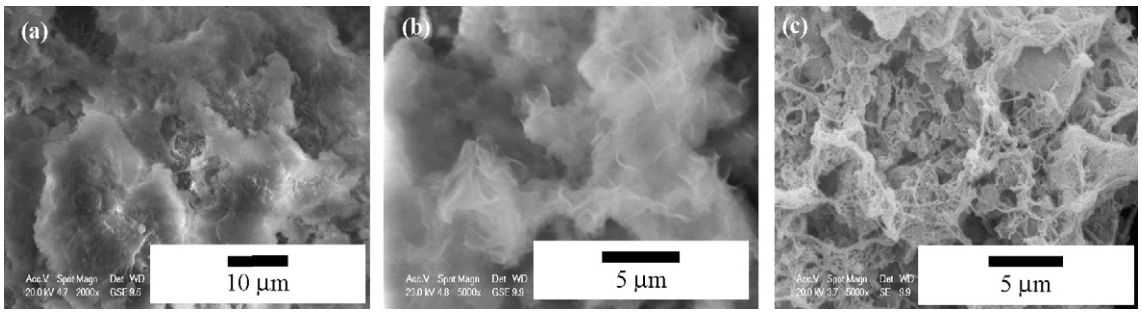

Fig. 9. Scanning electron microscope pictures of polyethylene from: (a) homogeneous catalyst [Zr{$Me_2Si(\eta^5$-$C_5Me_4)(\eta^5$-$C_5H_4)$}Cl_2], (b) SG/[Zr{$Me_2Si(\eta^5$-$C_5Me_4)(\eta^5$-$C_5H_4)$}Cl_2]/MAO and (c) MCM-41/[Zr{$Me_2Si(\eta^5$-$C_5Me_4)(\eta^5$-$C_5H_4)$}Cl_2]/MAO.

Scanning electron microscopy was employed in order to assess morphological differences between the three polyethylene samples obtained from the different systems ([Zr{$Me_2Si(\eta^5$-$C_5Me_4)(\eta^5$-$C_5H_4)$}Cl_2], SG/[Zr{$Me_2Si(\eta^5$-$C_5Me_4)(\eta^5$-$C_5H_4)$}Cl_2]/MAO and MCM-41/[Zr{$Me_2Si(\eta^5$-$C_5Me_4)(\eta^5$-$C_5H_4)$}Cl_2]/MAO), (Fig. 9). Inspection of the images reveals differences between the samples. The polymer produced by the homogeneous system (Fig. 9a) is sponge-like due most probably to the removal of solvent, and is not very different in aspect from the SG sample. However, the PE sample from the MCM-41 system takes on fibre morphology, due most likely to chains growing out of the MCM-41 channel aggregates.

4. Conclusions

The present study attempts to give a better understating of the behaviour, properties and structure of the supported metallocene catalysts in olefin polymerization. For this reason, a characterization of the samples MCM-41/[Zr{$Me_2Si(\eta^5$-$C_5Me_4)(\eta^5$-$C_5H_4)$}Cl_2] and MCM-41/[Zr{$Me_2Si(\eta^5$-$C_5Me_4)(\eta^5$-$C_5H_4)$}Cl_2]/MAO has been successfully carried out employing different techniques. MAS NMR spectroscopy shows that the metallocene fragment is bound to the support surface, and that a degradation product was formed after exposure to air. In terms of structural features, XRD analysis shows that the hexagonal pore structure of MCM-41 becomes less ordered after modification with MAO. The physical parameters of nitrogen isotherms indicate that the pores become slightly smaller as a result of the immobilization of zirconocene dichloride, but an exposure of the material to MAO resulted in N_2 adsorption/desorption isotherms that show the partial filling of the mesopores. MCM-41/metallocene/MAO catalysts **1**–**3** have been found to be less active in polymerization of ethylene than their SG analogues, although higher molecular weights are attained. Scanning electron microscope studies demonstrate that the *ansa*-metallocene complexes supported on MCM-41 follow, in the polymerization, the so-called replica phenomenon, and that the polyethylene takes on fibre morphology.

Acknowledgements

We gratefully acknowledge financial support from the Ministerio de Educación y Ciencia, Spain (CTQ2005-07918-C02-02/BQU), the Comunidad de Madrid and the Universidad Rey Juan Carlos (S-0505/PPQ-0328, URJC-CM-2006-CET-0568, URJC-CM-2007-CET-1491 and graduate fellowship for D.P.-C). We thank Dr. F. Carrillo-Hermosilla (Universidad de Castilla-La Mancha) for helpful discussions. We would also like to thank LATEP (Universidad Rey Juan Carlos) for their assistance in polymer analysis.

References

[1] D. Zhao, J. Feng, Q. Huo, N. Melosh, G.H. Fredrickson, B.F. Chmelka, G.D. Stucky, Science 279 (1998) 548.
[2] (a) R.J.P. Corriu, E. Lancelle-Beltran, A. Mehdi, C. Reyé, S. Brandés, R. Guilard, J. Mater. Chem. 12 (2002) 1355;
(b) Y. Kim, P. Kim, C. Kim, J. Yi, J. Mater. Chem. 13 (2003) 2353;
(c) W.M. van Rhijn, D.E. de Vos, W. Bossaert, J. Bullen, B. Wouters, P.A. Jacobs, Stud. Surf. Sci. Catal. 17 (1998) 183;
(d) D. Margolese, J.A. Melero, S.C. Christiansen, B.F. Chmelka, G.D. Stucky, Chem. Mater. 12 (2000) 2448;
(e) Y. Park, T. Kang, Y.S. Cho, J.C. Park, J. Yi, Stud. Surf. Sci. Catal. 146 (2003) 637;
(f) K. Mukhopadhyay, B.R. Sarkar, R.V. Chaudhari, J. Am. Chem. Soc. 124 (2002) 9692.
[3] C. Copéret, M. Chabanas, R. Petroff Saint-Arroman, J.-M. Basset, Angew. Chem. Int. Ed. 42 (2003), 156 and references therein.
[4] (a) P.W.N.M. van Leeuwen, Homogeneous Catalysis: Understanding the Art, Springer, Heidelberg, 2004;
(b) B. Cornils, W.A. Hermann, Applied Homogeneous Catalysis with Organometallic Compounds, Wiley–VCH, Weinheim, 1996.
[5] (a) W. Kaminsky, Macromol. Chem. Phys. 197 (1996) 3907;
(b) W. Kaminsky, M. Arndt, Adv. Polym. Sci. 127 (1997) 143.
[6] (a) P. Roos, G.B. Meier, J.J.C. Samson, G. Weicker, K.R. Westerterp, Macromol. Rapid Commun. 18 (1997) 319;
(b) W. Kaminsky, D. Arrowsmith, C. Strübel, J. Polym. Sci. Part A: Polym. Chem. 37 (1999) 2959;

(c) R. Goertzki, G. Fink, B. Tesche, B. Steinmetz, R. Rieger, W. Uzick, J. Polym. Sci. Part A: Polym. Chem. 37 (1999) 677.
[7] (a) S. Collins, W.M. Kelly, D.A. Holden, Macromolecules 25 (1992) 1780;
(b) K. Soga, M. Kaminaka, Makromol. Chem. Phys. 195 (1994) 1369;
(c) K. Soga, H. Kim, T. Shiono, Makromol. Chem. Phys. 195 (1994) 3341.
[8] D.-H. Lee, K.-B. Yoon, Macromol. Rapid Commun. 18 (1997) 427.
[9] (a) C.T. Kresge, M.E. Leonowicz, W.J. Roth, J.C. Vartulli, J.S. Beck, Nature 359 (1992) 710;
(b) P. Behrens, Adv. Mater. 5 (1993) 127;
(c) C.-Y. Chen, H.-X. Li, M.E. Davis, Micropor. Mater. 2 (1993) 17;
(d) A. Sayari, I. Moudrakovski, J.S. Reddy, C.I. Ratcliffe, J.A. Ripmeester, K.F. Preston, Chem. Mater. 8 (1996) 2080.
[10] (a) Y.S. Koo, T.K. Han, J.W. Park, S.I. Woo, Macromol. Rapid Commun. 17 (1996) 749;
(b) S.K. Woo, Y.S. Ko, T.K. Han, J.W. Park, in: A. Togni, R.L. Halterman (Eds.), Metallocenes, Wiley, New York, 1996, pp. 271–292.
[11] (a) S. Gómez-Ruiz, S. Prashar, L.F. Sánchez-Barba, D. Polo-Cerón, M. Fajardo, A. Antiñolo, A. Otero, M.A. Maestro, C.J. Pastor, J. Mol. Catal. A: Chem. 264 (2007) 260;
(b) D. Polo-Cerón, S. Gómez-Ruiz, S. Prashar, M. Fajardo, A. Antiñolo, A. Otero, I. López-Solera, M.L. Reyes, J. Mol. Catal. A: Chem. 268 (2007) 264;
(c) D. Polo-Cerón, S. Gómez-Ruiz, S. Prashar, M. Fajardo, A. Antiñolo, A. Otero, Collect. Czech. Chem. Commun. 72 (2007) 747.
[12] (a) C. Alonso, A. Antiñolo, F. Carrillo-Hermosilla, P. Carrión, A. Otero, J. Sancho, E. Villaseñor, J. Mol. Catal. A: Chem. 220 (2004) 286;
(b) C. Alonso-Moreno, A. Antiñolo, F. Carrillo-Hermosilla, P. Carrión, I. López-Solera, A. Otero, S. Prashar, J. Sancho, Eur. J. Inorg. Chem. (2005) 2924;
(c) P. Carrión, F. Carrillo-Hermosilla, C. Alonso-Moreno, A. Otero, J. Antiñolo, E. Sancho, Villasenor, J. Mol. Catal. A: Chem. 258 (2006) 236.
[13] (a) D. Pérez-Quintanilla, A. Sánchez, I. del Hierro, M. Fajardo, I. Sierra, J. Colloid Interf. Sci. 313 (2007) 551;
(b) Y. Pérez, D. Pérez-Quintanilla, M. Fajardo, I. Sierra, I. del Hierro, J. Mol. Catal. A: Chem. 271 (2007) 227.
[14] M.V. Landau, S.P. Varkey, M. Herskowitz, O. Regev, S. Pevzner, T. Sen, Z. Luz, Micropor. Mesopor. Mater. 33 (1999) 149.
[15] (a) A. Antiñolo, I. López-Solera, I. Orive, A. Otero, S. Prashar, A.M. Rodríguez, E. Villaseñor, Organometallics 20 (2001) 71;
(b) A. Antiñolo, I. López-Solera, A. Otero, S. Prashar, A.M. Rodríguez, E. Villaseñor, Organometallics 21 (2002) 2460.
[16] K. Kageyama, J.I. Tamazawa, T. Aida, Science 285 (1999) 2113.
[17] G. Braca, G. Sbrana, A.M. Raspolli-Galleti, A. Altomare, G. Arribas, M. Michelotti, F. Ciardelli, J. Mol. Catal. A: Chem. 107 (1996) 113.
[18] M. Michelloti, A. Altomare, F. Ciardelli, E. Roland, J. Mol. Catal. A: Chem. 129 (1998) 241.
[19] H. Rahiala, I. Beurroies, T. Eklund, K. Hakala, R. Gougeon, P. Trens, J.B. Rosenholm, J. Catal. 188 (1999) 14.
[20] W. Kaminsky, C. Strübel, H. Lechert, D. Genske, S.I. Woo, Macromol. Rapid Commun. 21 (2000) 909.
[21] (a) Z.B. Ye, S.P. Zhu, W.J. Wang, H. Alsyouri, Y.S. Lin, J. Polym. Sci., Part B: Polym. Phys. 41 (2003) 2433;
(b) X.C. Dong, L. Wang, W.Q. Wang, H.J. Yu, J.F. Wang, T. Chen, Z.R. Zhao, Eur. Polym. J. 41 (2005) 797.
[22] (a) F. Silveira, S.R. Loureiro, G.B. de Galland, F.C. Stedile, J.H.Z. dos Santos, T. Teranishi, J. Mol. Catal. A: Chem. 206 (2003) 289;
(b) S. Rodrigues, F. Silveira, J.H.Z. dos Santos, M.L. Ferreira, J. Mol. Catal. A: Chem. 216 (2004) 19;
(c) F. Silveira, G.P. Pires, C.F. Petry, D. Pozebon, F. Stedile, J.H.Z. dos Santos, A. Rigacci, J. Mol. Catal. A: Chem. 265 (2007) 167.
[23] (a) L.K. Van Looveren, D.E. de Vos, K.A. Vercruysse, D.F. Geysen, B. Janssen, P.A. Jacobs, Catal. Lett. 56 (1998) 53;
(b) L.K. Van Looveren, D.F. Geysen, D.A. Vercruysse, B.H. Wouters, P.J. Grobet, P.A. Jacobs, Angew. Chem. Int. Ed. 37 (1998) 517.
[24] J. Tudor, D. O'Hare, Chem. Commun. (1997) 603.
[25] A. Corma, J. Phys. Chem. 99 (1995) 1023.
[26] L. Reven, J. Mol. Catal. 86 (1994) 447.
[27] J. Turunen, T.T. Pakkanen, B. Löfgren, J. Mol. Catal. A: Chem. 123 (1997) 35.
[28] J.S. Beck, J.C. Vartulli, W.J. Roth, M.E. Leonowicz, C.T. Kresge, K.D. Smith, C.T.-W. Chu, D.H. Olson, E.W. Sheppard, S.B. McCullen, J.B. Higgins, J.L. Schlenker, J. Am. Chem. Soc. 114 (1992) 10834.
[29] (a) A. Corma, J. Catal. 148 (1994) 569;
(b) M. Busio, J. Jänchen, J.H.C. Hooff, Micropor. Mater. 5 (1995) 211;
(c) A.A. Romero, M.D. Alba, J. Klinowski, J. Phys. Chem. B 102 (1998) 123.
[30] K.S.W. Sing, D.H. Everett, R.A.W. Haul, L. Moscou, R.A. Pierotti, J. Rouquérol, T. Siemieniewska, Pure Appl. Chem. 57 (1985) 603.
[31] D. Zhao, Q. Huo, J. Feng, B.F. Chmelka, G.D. Stucky, J. Am. Chem. Soc. 120 (1998) 6024.
[32] B.A. Morrow, Stud. Surf. Sci. Catal. 57 (1990) 161.
[33] M.C. Haag, C. Krug, J. Dupont, G. Barrera, J.H.Z. dos Santos, T. Uozumi, T. Sano, K. Soga, J. Mol. Catal. A: Chem. 169 (2001) 275.
[34] L.T. Zhuraviev, Colloids Surf. A 74 (1993) 71.
[35] F.W. Billmeyer, Textbook of Polymer Science, Wiley, New York, 1984, pp. 332–366.
[36] M.C. Sacchi, D. Zucchi, J. Tritto, P. Locatelli, T. Dall'Occo, Macromol. Rapid Commun. 16 (1995) 581.
[37] J.H.Z. dos Santos, C. Drug, M.B. da Rosa, F.C. Stedile, J. Dupont, M.M.C. Forte, J. Mol. Catal. A: Chem. 139 (1999) 199.
[38] J.R. Severn, J.C. Chadwick, R. Duchateau, N. Friederichs, Chem. Rev. 105 (2005) 4073.
[39] S.I. Woo, Y.S. Ko, T.K. Han, Macromol. Chem. Phys. 16 (1995) 489.
[40] K.-S. Lee, C.-G. Oh, J.-H. Yim, S.-K. Ihm, J. Mol. Catal. A: Chem. 159 (2000) 301.
[41] (a) Y.S. Ko, S.I. Woo, Macromol. Chem. Phys. 202 (2001) 5;
(b) N. Millot, C.C. Santini, A. Baudouin, J.-M. Basset, Chem. Commun. (2003) 2034;
(c) X. Dong, L. Wang, G. Jiang, Z. Zhao, T. Sun, H. Yu, W. Wang, J. Mol. Catal. A: Chem. 240 (2005) 239.
[42] Y.S. Ko, T.K. Han, J.W. Park, S.I. Woo, Macromol. Rapid Commun. 17 (1996) 749.
[43] J.L. Brinen, A.N. Speca, K. Tormaschi, K.A. Russell, US Pat. 5,665,665 (1997).